

Published in final edited form as:

Hum Brain Mapp. 2006 April ; 27(4): 325–339. doi:10.1002/hbm.20188.

Reading Embossed Capital Letters: An fMRI Study in Blind and Sighted Individuals

H. Burton^{1,2,*}, D.G. McLaren¹, and R.J. Sinclair¹

¹Department of Anatomy and Neurobiology, Washington University School of Medicine, St. Louis, Missouri

²Department of Radiology, Washington University School of Medicine, St. Louis, Missouri

Abstract

Reading Braille activates visual cortex in blind people [Burton et al., *J Neurophysiol* 2002;87: 589-611; Sadato et al., *Nature* 1996;380:526-528; Sadato et al., *Brain* 1998;121:1213-1229]. Because learning Braille requires extensive training, we had sighted and blind people read raised block capital letters to determine whether all groups engage visual cortex similarly when reading by touch. Letters were passively rubbed across the right index finger at 30 mm/s using an MR-compatible drum stimulator. Age-matched sighted, early blind (lost sight 0–5 years), and late blind (lost sight >5.5 years) volunteers performed three tasks: stating an identified letter, stating a verb containing an identified letter, and feeling a moving smooth surface. Responses were voiced immediately after the drum stopped moving across the fingertip. All groups showed increased activity in visual areas V1 and V2 during both letter identification tasks. Blind compared to sighted participants showed greater activation increases predominantly in the parafoveal-peripheral portions of visuotopic areas and posterior parts of BA 20 and 37. Sighted participants showed suppressed activity in most of the same areas except for small positive responses bilaterally in V1, left V5/MT+, and bilaterally in BA 37/20. Blind individuals showed suppression of the language areas in the frontal cortex, while sighted individuals showed slight positive responses. Early blind showed a more extensive distribution of activity in superior temporal sulcal multisensory areas. These results show cross-modal reorganization of visual cortex and altered response dynamics in nonvisual areas that plausibly reflect mechanisms for adaptive plasticity in blindness.

Keywords

blindness; human; magnetic resonance imaging; visual cortex; physiology

INTRODUCTION

Imaging studies (PET and functional MRI) have shown that a range of tasks activate visual cortex in blind people [Aleman et al., 2001; Amedi et al., 2003; Arno et al., 2001; Büchel et al., 1998; Burton et al., 2002a,b, 2003, 2004; Gizewski et al., 2003; Gougoux et al., 2005; Kujala et al., 2005; Lambert et al., 2004; Röder et al., 2001, 2002; Sadato et al., 1996, 1998, 2002; Vanlierde et al., 2003; Zatorre, 2001]. Unfortunately, there has been little evidence of domain selective functional specificity aside from the observation that linguistic tasks

preferentially activated left visual areas in blind people. The principle of parsimony would suggest that cross-modal reorganization ought to be contingent on existing visual cortex architecture. Consistent with this notion are developmental findings in monkeys that showed little structural alteration in the gray matter of area 17 following binocular enucleations that were placed after the gestational stage for cortical cell proliferation and migration [Rakic, 1988]. Most congenitally blind people have no sight due to late gestational events like retinopathy of prematurity. Consequently, we hypothesized that most early blind individuals have a genetically predetermined visual cortex architecture that at birth resembles the organization in sighted people. Adventitiously blind individuals have visual deprivation imposed on normal visual cortex architecture.

Given the idea that reorganized visual cortex in blind people probably reflects normal visual cortex cytoarchitecture, an overriding issue is to determine what functional properties persist. An important characteristic of visual cortex in sighted people is domain specialization wherein unique functional activity has been found in anatomically identifiable regions [Grill-Spector and Malach, 2004]. Domain specializations dedicated to visual features like color or disparity are unlikely to function similarly in blindness. A more probable hypothesis, however, is that the functional specialization described for object-selective regions in dorsal occipito-temporal (DOT) and ventral occipito-temporal (VOT) cortex [Hasson et al., 2002] persists in blind people. In sighted people distinct partitions in DOT and VOT are selectively activated when processing visual information from different kinds of objects. A useful characteristic of the different object domains is their relationship to eccentricity band representations readily demonstrated in highly visuotopic lower tier visual areas [Hasson et al., 2002, 2003]. Thus, regions preferentially activated when viewing faces or letters associate with foveal eccentricities; cortex activated by objects relate to parafoveal eccentricities; and cortex selectively engaged when viewing items on buildings or in scenes link to peripheral eccentricities [Hasson et al., 2002, 2003]. The question is whether the global nature of object selective domain specialization is applicable to adaptive visual cortex reorganization in blindness. In the present study we sought to assess this notion by examining the distribution of activated regions during a tactile discrimination task and by relating these regions in blind people to anatomical correlates of object selective regions previously defined in sighted people.

We utilized a tactile-based language task to determine whether selective lower and higher tier visual areas were activated in sighted and blind people. Prior studies [Büchel et al., 1998; Burton et al., 2002a; Melzer et al., 2001; Sadato et al., 1996, 1998] showed extensive engagement of visual areas with tactile reading in blind people. In higher tier visual areas we especially assessed whether the domains activated in occipitotemporal cortex were confined to specific components of object selective functional regions previously studied in sighted people when they viewed visual images of objects compared to textures [Hasson et al., 2002, 2003; Kanwisher et al., 1997; Levy et al., 2001, 2004; Malach et al., 1995, 2002; Yovel and Kanwisher, 2004]. Based on prior studies that have described different activation patterns in lower and higher tier visual areas in early- and late-onset blind Braille readers [Büchel et al., 1998; Burton et al., 2002a; Melzer et al., 2001; Sadato et al., 1996, 1998], we expected similar differences between blind groups in the present study across all visual areas.

Assessing the effects of tactile reading by training sighted people to read Braille is prohibitive [Loomis, 1981; Uhl et al., 1991]. However, block capital letters can be readily identified through touch [Loomis, 1981; Vega-Bermudez et al., 1991] and performance accuracy is not affected when the letters are passively rubbed across a fingertip [Vega-Bermudez et al., 1991]. Thus, in the present study raised letters were applied passively to all participants, which eliminated probable confounds from the considerable tactile scanning skills blind people must acquire when learning Braille [Millar, 1997].

SUBJECTS AND METHODS

Participants

Nine individuals (four female) categorized as early blind (EB) had no sight at birth or lost sight before learning to read print (blindness onset: before ~5 years). Nine individuals (six female) categorized as late blind (LB) lost sight after learning to read print (blindness onset: 5.5–41 years). Ten normally sighted (NS) individuals (three female) matched the two groups of blind people by age. All participants provided informed consent following guidelines approved by the Human Studies Committee of Washington University. Table I presents demographic characteristics of all participants and lists identification numbers, which were retained for blind people who had participated in previous studies [Burton et al., 2002a,b, 2003, 2004]. Except for ophthalmologic causes of blindness (Table I), all participants were free from neurological disease and had normal brain anatomy as assessed from structural images by an experienced neuroanatomist. All blind participants were Braille literate with reading speeds between 10–182 wpm (Table I) and stated that they were familiar with block capital letters. Four EB and six LB participants self-reported light sensitivity, but none could read print or navigate without aid. Responses to a modified Edinburgh handedness inventory indicated that right-handedness predominated across groups [Raczkowski et al., 1974]. However, four blind participants read Braille exclusively with their left hands (2 EB, 2 LB), three read with their right (1 EB, 2 LB), and the remainder used both hands (Table I).

Experimental Setup

During scanning embossed capital letters were passively rubbed against the right index fingertip from the proximal to distal end using a rotating drum device (Fig. 1), which was constructed with two fiberglass wheels and a connecting belt (Fig. 1A). A finger/hand rest (Fig. 1B) aligned the finger over a selected track on the belt. The 330-cm belt consisted of a flexible photopolymer printing material that was embossed with block capital letters (A, I, J, L, O, T, U, and W) using a commercial photo etching process (B.W. Johnson, Joplin, MO). Letters (Arial font) were 8 mm high, variable width respective to the letter (e.g., W is wider than U), and were raised ~0.8 mm. These letters were selected because they are least confusable [Vega-Bermudez et al., 1991]. There were five tracks, each containing a different random sequence of 19 letter strings. Letter strings were 13.5 cm long and contained six identical letters.

Prior to scanning, letter strings identical to those described above were used to familiarize participants with the stimuli. Participants stated the letter they felt after they actively rubbed their right index finger down each string of six letters. Participants were immediately told what the letter was if the answer was incorrect. Letter strings were randomly presented until all letters were correctly identified. Additional letter strings were then presented passively, until all letters were identified correctly, to simulate the actual stimuli in the scanner. Participants did not see the letters/letter strings until after all scanning sessions.

Rotation was driven by a stepping motor attached to the wheel located at the end of the scanner bed. An optical encoder (Computer Optical Products, Chatsworth, CA, Model CP-250-1024-8mm) on the drive motor axle transmitted position information. Shielded cables connected power to the motor and transducer signals to an interface circuit through a grounded filter-plate that separates the scanner room from an adjacent control room. On-off cycles of drum rotation were synchronized to image acquisition cycles using scanner pulses at the beginning of TR intervals. MRI experiments with phantoms demonstrated that the drum device did not introduce noise into structural or functional images.

A letter event involved translating a letter string under the finger at 30 mm/s and then having participants overtly respond during a pause in rotation. Stimulation and responses lasted

~7.5 s (3 frames). Letter string events were presented using an event-related, jittered design that was based on a truncated negative exponential distribution of intervals. Event-to-event onset ranged from 15-27.5 s (6-11 frames). Each session lasted 154 frames (~6.4 min) and included 2 frames that were discarded for magnetization equilibrium, 5 initial and 5 end frames for baseline measurements, and 19 events of 8 frames each. Participants stated the identified letter in scanning sessions 2 and 3 (OL task) and stated a verb that contained the identified letter in scanning sessions 4 and 5 (OW task). There was no advance warning for the word task except for instructions just prior to scanning, which prevented possible rehearsal of words during the letter identification task. Participants were instructed to identify a verb that contained the letter in any location in the word and to say a different verb for each letter string. The first and last scanning sessions were controls when participants felt only a moving smooth surface that was rotated with the same timing of rotations and jittered pauses used during letter string events (BL task). We instructed participants to keep their fingers in contact with the drum surface during control imaging sessions; they were also told that no discriminations were required during these scans. The two sessions per task resulted in 38 events per event-type for each participant.

Verbal responses were digitally recorded using commercial software (Sony, SoundForge) and an MR compatible microphone (RTI, Northridge, CA). We used an adaptive spectral subtraction algorithm, optimized for each subject to remove MR gradient noise [Nelles et al., 2003]. The processed signal contained clear verbal responses and allowed extraction of reaction times (Table I, RT letters and RT words) based on the peak of the response for all letter and word trials and relative to the end of rotation of each letter string. Percentage correct responses and reaction time data were obtained only from some participants (see Table I) because of occasional technical problems.

All participants were blindfolded and instructed to close their eyes during functional imaging sessions. Lights were turned on between scans and all participants were instructed to open their eyes. Sighted participants reported detecting light at the edges of their blindfolds during these between-scan intervals.

MRI Acquisition and Reconstruction

We acquired images with a Siemens (Erlangen, Germany) 3 T Allegra scanner and a standard birdcage headcoil within which the head was immobilized by a vacuum pillow. Structural images were acquired using a T_1 -weighted sagittal magnetization-prepared rapid acquisition gradient echo (MP-RAGE) (repetition time (TR) = 2,100 msec; echo time (TE) = 3.93 msec; flip angle = 7° ; inversion time (TI) = 1,000 msec; $1 \times 1 \times 1.25$ mm). Functional images were collected using a Siemens single-shot, gradient echo echo-planar imaging (EPI) sequence optimized for blood oxygen level-dependent (BOLD) contrast (T_2^*) (TR = 2,500 msec; TE = 30 msec; flip angle = 90°). Functional images were acquired with 32 contiguous 4-mm slices parallel to the AC-PC plane, with an in-plane resolution of 4×4 mm, and were automatically prescribed based on computed registration of a coarse sagittal MP-RAGE T_1 -weighted sequence (TR = 722 msec; TE = 3.93 msec; flip angle = 8° ; TI = 380 msec; $2 \times 2 \times 2$ mm) to an atlas representative target image [Mugler and Brookeman, 1990]. Additionally, structural T_2 -weighted (T2W) spin echo (SE) images (TR = 8,430 msec; TE = 98 msec; $1.33 \times 1.33 \times 3$ mm) were acquired in the same plane as the EPI images to facilitate alignment of the functional images to atlas space [Talairach and Tournoux, 1988].

Functional data passed through several unsupervised steps to compensate for asynchronous slice acquisition, remove systematic odd vs. even slice intensity differences due to imperfect slice excitation profiles that result from contiguous, interleaved slice acquisition, and to realign within and across runs using difference image variance minimization to compensate for head movements [Friston et al., 1995a; Snyder, 1996]. Compensation was achieved

through a single resampling of functional volumes using fast 3D cubic spline interpolation, which produced results very similar to those obtained by sinc interpolation [Hajnal et al., 1995].

Our atlas representative target conforms to the Talairach system [Talairach and Tournoux, 1988] as defined by the SN procedure [Lancaster et al., 1995]. The target template was produced by mutual coregistration (12 parameter affine warp) of MP-RAGE images from 12 normal, young adults. Atlas transformation of functional (EPI) data was achieved by computing a sequence of affine transforms as follows: EPI \rightarrow T2W \rightarrow MP-RAGE \rightarrow atlas representative target. T2W is a conventional T_2 -weighted image, the inclusion of which minimized systematic EPI \rightarrow MP-RAGE registration errors caused by EPI distortion and susceptibility artifacts [Ojemann et al., 1997]. Slice plane stretch in addition to rigid body motion (6 parameters) partially compensated for EPI distortion and accomplished cross-modal registration using an in-house variant of the method of Andersson et al. [1995]. This procedure required no editing of extracranial structures and performed with precision comparable to or better than AIR [Woods et al., 1993]. Algebraic composition of transforms (matrix multiplication) generated the functional EPI \rightarrow atlas transform. Reslicing the functional data (or any intermediate image) in register with the atlas then involved only one interpolation. All statistical analyses were conducted in an atlas space of 2 mm^3 and after spatial smoothing (4 mm FWHM).

Statistical Analyses

We examined results from individuals and groups. A voxel-wise general linear model (GLM) [Miezin et al., 2000; Ollinger et al., 2001a,b] was used to estimate the BOLD responses for each event-type (OL, OW, or BL) and for each participant without assuming a hemodynamic response function [Dale and Buckner, 1997; Miezin et al., 2000; Ollinger et al., 2001a,b]. The model included terms per imaging session for an intercept (baseline), linear trend, and temporal high-pass filter (0.014 Hz). Responses were estimated over a 20-s interval (8 frames) beginning at event onset; thus, our model included eight terms for each event-type representing each frame of the response. Estimated event-type time courses are relative to the estimated baseline. Next, we computed z -statistic maps for each event-type per participant. For this analysis we cross-correlated the estimated BOLD responses per voxel with an assumed hemodynamic response function (HRF), which was a delayed gamma function (2-s delay) [Boynton et al., 1996] convolved with the stimulus duration (3 frames, 0–7.5 s). Residuals from this fit were used to obtain t -statistics per voxel [Friston et al., 1995b; Zarahn et al., 1997]. We converted t -statistic maps for each individual to equally probable z -scores that were thresholded on the basis of Monte Carlo simulations [Forman et al., 1995] at a multiple-comparisons corrected false-detection rate of $P = 0.05$ ($z = 4$ over at least six contiguous, face-connected voxels). Inspection of these maps established the pattern of activity in individual participants (e.g., Fig. 3).

Group differences in BOLD responses were assessed using a repeated measures, mixed effects ANOVA, treating participants as a random factor and time (8 frames), event-type (OL, OW, and BL), and group (EB, LB, and NS) as fixed factors. The ANOVA computed main effects of time, event-type, group, and the associated interactions. The dependent variable of percent MR signal change per voxel was calculated using estimates from the GLM obtained from each participant. F-ratios for each factor in the ANOVA models were converted to z -scores whose degrees of freedom were adjusted for covariance (sphericity correction) and thresholded on the basis of Monte-Carlo simulations at $P = 0.05$ ($z = 3$ over at least 45 contiguous, face-connected voxels) (insimulations on random noise patterns similar to the method described by Forman et al. [1995]).

Statistical maps based on the time-by-group interaction factor identified voxels in which response profiles differed between groups. These maps were projected onto a population-average, landmark, and surface-based atlas (PALS) [Van Essen, 2005] to facilitate evaluation of cortical differences between groups. Functional data were projected by assigning voxel-based z -score values to the associated surface nodes in 12 normal individuals. The average of each node was displayed on PALS. The PALS atlas includes boundary definitions for Brodmann areas and visuotopic and nonvisuotopic visual areas and eccentricity bands within lower tier visual areas.

Regional analysis increases the statistical power of selected contrasts beyond that obtained with voxel-based methods by reducing the multicomparison correction applied to significance thresholds. Regions of interest (ROIs) were objectively defined using two steps. First, the z -score maps from the ANOVA were subdivided into volume-based reconstructions representing each visuotopic area or selected Brodmann area (BA) in the PALS atlas. Visuotopic area volumes and BA volumes were defined by projecting the surface representation to volume space assuming 3-mm thick cortex [Van Essen, 2005]. The ANOVA statistical maps retained within each specified volume were submitted to a peak localization algorithm. Peaks closer than a specified radius were consolidated, based on a center-of-mass calculation, and spheres drawn around each remaining peak such that no voxels were excluded from the analysis and enough voxels were included to account for individual anatomical variation.¹ Through a second conjunction the domains of the resulting spheres were constrained to conform to the anatomy of the PALS volumes. This served to confine objectively defined voxels to those located wholly within a specified visual area or BA. For regions in the occipital or frontal cortex, multiple spheres were collapsed within each anatomical volume to create a single ROI. In BA 22 several regions were identified. Our peak search algorithm also identified the peak Talairach atlas coordinates [Talairach and Tournoux, 1988] within each anatomical volume (Tables II/III), based on a center-of-mass calculation (as described above).

Participant time courses were extracted for each ROI; the time course values were DC shift corrected for each event-type, for each participant, and for each ROI. Group averages and SEM were plotted per event-type in each ROI (Figs. 5, 6). Response time courses differed in shape and magnitude for different groups and event-types. As a consequence, group and event-type differences were assessed with multivariate F-tests in which MR percent signal change from time course intervals were entered as dependent variables into a repeated measures region-wise MANOVA (PROC GLM, Statistical Analysis Software v. 9.1, SAS Institute, Cary, NC). The MANOVA makes no assumptions about the shape of the BOLD response. To obtain repeated measures of time courses, the GLM procedures described above were used to estimate BOLD responses separately for each session, thereby providing two measures per participant for each event-type (OL, OW, or BL). Participant time courses were extracted for each ROI and DC shift-corrected for each event-type and session. A repeated measures region-wise MANOVA was run for each pairing of groups per event-type (i.e., EB-OL vs. LB-OL), and OL vs. OW per group. The probability of the exact F-statistic from Wilks' Lambda was used for decisions of significant differences between groups and event-types ($P < 0.05$).

¹The specified distance between peaks and sphere radius varied from lobe to lobe. Occipital cortex had a specified distance of 6 mm and a sphere with a radius of 10 mm. Frontal cortex had a specified distance of 7 mm and sphere with a radius of 12 mm. Temporal cortex had a specified distance of 10 mm and sphere with a radius of 10 mm. Different parameters were used to optimize region definitions. Overlapping spheres were divided at the plane midway between the peaks. Contract grant sponsor: National Institutes of Health (NIH); Contract grant number: NS37237.

RESULTS

Task Performance

Accuracy in identifying the letters was similar across all groups and averaged >85% (Fig. 2A, Table I). RTs differed between groups only for the OL, but not the OW task (Fig. 2B). These differences were due to significantly faster RTs in EB to the OL task. RTs were slower for the OW task and differed significantly from RTs for the OL task in EB and NS groups.

Occipital Visual Areas

Pericalcarine sulcal cortex, V1—Positive BOLD responses were noted bilaterally in the posterior pole of the occipital cortex (Talairach coordinate: $Y < -87$) for the majority of sighted (9/10) and blind (7/9 EB, 8/9 LB) participants. As shown in Figure 3, activation increases occupied pericalcarine, adjacent cuneus, and lingual gyral cortex. The identified cortex has been defined as visual areas V1 and V2 in sighted people. No group differences were found in the posterior parts of V1/V2 (Fig. 4A,J). Further anterior, however, the ANOVA results showed significant group differences from pericalcarine and immediately adjacent cortex that involved left V1 dorsal (Fig. 4C, $Y = -85$), left V2 dorsal (Fig. 4B, $Y = -89$), and right V1 dorsal and ventral (Fig. 4D, $Y = -79$) (Table II). This portion of V1 and V2 normally corresponds to the parafoveal eccentricities ($4-12^\circ$) (Fig. 4K) [Hasson et al., 2002]. Bilaterally in this more anterior part of V1d, EB and LB had time courses that differed significantly from those in NS during OL and OW tasks (Table II). The MANOVA indicated similar results for V2d (Table II). For V1d, Figure 5 illustrates that these differences arose from greater positive BOLD responses during the OL and OW tasks in the blind groups. The responses were generally uniform, with single peaks even in the NS group during the OL and OW tasks. The appearance of biphasic responses during the OL task resulted from variant responses in a few blind participants.

Cuneus and middle/superior occipital gyri (SOG and MOG), V3/V3a—

Extrastriate visual areas superior to the calcarine sulcus were bilaterally activated during OL and OW tasks in blind participants. Significant group differences in the ANOVA were located in the cuneus, SOG, and superior MOG, areas that have been defined as V3 and V3a in sighted people (Fig. 4A, $Y = -95$; 4J). This part of cortex primarily corresponds to the parafoveal-peripheral ($4-90^\circ$) eccentricity bands for V3 on the left and foveal-parafoveal ($0-12^\circ$) bands on the right and bilaterally for V3a (Fig. 4J,K). EB and LB had time courses that differed significantly from those in NS during all tasks in the identified parts of V3/V3a (Table II). For V3 and V3a, Figure 5 illustrates, especially during the OL and OW tasks, that these response differences were due to greater positive BOLD responses in both blind groups compared to slightly negative late responses in the NS group. Similar group differences were found during the BL task despite generally smaller responses. The appearance of biphasic responses during the OL task resulted from variant responses in a few blind participants.

Lingual and posterior fusiform gyri, VP, V4v—The ANOVA indicated significant group differences across the inferior surface of occipital cortex (Fig. 4D–G); the extrastriate lower tier visual areas located inferior to the calcarine sulcus have been defined as VP and V4v in sighted people (Fig. 4J). The identified cortex occupied more of the parafoveal-peripheral eccentricity bands on the left and peripheral eccentricity band on the right (Fig. 4J,K). Bilaterally, responses in VP and V4v showed significantly different positive BOLD responses in EB and LB during all tasks compared to slight negative responses in NS (Fig. 5, VP, V4v; Table II).

Trans-occipital sulcus, V7—The ANOVA indicated significant group differences in cortex that mostly straddled the trans-occipital sulcus between SOG and MOG, an area that partly involves cortex defined as V7 in sighted people (Fig. 4B,C, $Y = -89, -85$). Positive BOLD responses during the BL and OL in EB differed significantly from negative responses in NS bilaterally (Fig. 5, V7, and Table II). Similar response differences were found between LB and NS bilaterally during BL and OW tasks and on the right during the OL task (Fig. 5, V7, and Table II).

Dorsal and Ventral Occipito-Temporal Cortex (DOT and VOT)

The cortex defined as DOT by Hasson et al. [2002, Hasson et al. 2003] (Fig. 4K) includes defined visual areas LOC and V5/MT+ and adjoining nonvisuotopic parts of BA 19. The cortex defined as VOT contains parts of visual area V8 and posterior BA 37 and 20 where these areas adjoin anteriorly to visuotopic visual areas [Van Essen, 2004].

MOG, LOC—The ANOVA indicated significant group differences within MOG bilaterally (Fig. 4C,D), an area that has been defined as LOC in sighted people (Fig. 4J). The identified cortex was similar bilaterally and occupied most of the defined LOC area (Table II, Fig. 4J). LOC bilaterally showed significantly different positive BOLD responses in both blind groups compared to slight negative responses in NS during all tasks (Fig. 5, LOC, and Table II).

Posterior inferior temporal sulcus (OpITS)/ascending limb of ITS, V5/MT+—Significant bilateral group differences were found anterior and slightly inferior to LOC and at the junction with pITS (Fig. 4D,E). This area has been defined as V5/MT+ in sighted people (Fig. 4J) [Dumoulin et al., 2000]. On the left all groups showed positive BOLD responses during all tasks, but on the right only the blind participants had positive responses for all tasks with larger magnitudes during OL and OW tasks compared to those in NS (Fig. 5, V5/MT+). On the left only the larger responses in EB differed significantly from those in NS; on the right positive responses from EB and LB differed from negative responses in NS for all tasks (Fig. 5, V5/MT+, Table II).

Fusiform gyrus (FG), V8—The ANOVA indicated significant group differences in the posterior FG (Fig. 4C,D), an area that has been defined as V8 in sighted people (Fig. 4J). Bilaterally, responses in V8 of EB and LB showed significantly different positive BOLD responses during all tasks compared to slight negative responses in NS (Fig. 5, V8, and Table II).

Anterior fusiform gyrus, BA 37 and BA 20—The ANOVA maps for group differences indicated bilateral regions in anterior and medial fusiform gyri (Fig. 4E–I) and an adjoining region in the right lateral fusiform gyrus (Fig. 4J), cortex in posterior BA 37 and 20 that has been identified as nonvisuotopic visual areas [Van Essen, 2004]. No significant group differences were noted in a left lateral fusiform gyrus region. Sighted and blind participants showed positive BOLD responses bilaterally in BA 37 (Fig. 5, BA 37). The MANOVA indicated that responses in EB differed significantly from those in NS during both letter tasks (Table II). Responses in LB and NS did not differ (Fig. 5, BA 37, and Table II). The MANOVA results for BA 20 were similar to those for BA 37 (Table II).

Visual Areas: Early vs. Late Blind

The responses in EB differed significantly from those in LB in several left visual areas (Table II, V2v, V3, V3a, V7, VP, V4v, and LOC) and a smaller number of right areas (Table II, V2d, V3, BA 37). EB showed larger positive responses compared to those in LB in nearly all of these areas (Fig. 5).

Superior Temporal Cortex

BA 22—The ANOVA map indicated group differences in bilateral superior temporal sulcus/gyrus regions (Fig. 6A,B), an area that has been defined as part of BA 22. The left hemisphere contained a single region where all groups showed positive BOLD responses during the OL and OW tasks (Fig. 6C). There were no responses during the BL task in any group. The right hemisphere had three anterior to posterior foci (Fig. 6B shows the anterior and posterior foci). Positive responses for the two most posterior regions were found in all groups (Fig. 6C), while only EB had positive responses in the most anterior region for OL and OW tasks (Fig. 6D). The EB responses differed significantly from NS and LB during the OL and OW tasks in nearly all of these regions (Table III). The responses in LB and NS were similar in these same regions (Fig. 6C,D, Table III). These MANOVA findings likely reflected larger and earlier response peaks during, especially the OL task, for EB compared to the responses in LB and NS (Fig. 6C,D).

Frontal Cortex (Language Areas)

Group differences in responses were located bilaterally in the inferior and middle frontal gyri, an area defined as part of BA 44, 46, and 47 on the left and 44, 45, and 46 on the right (Fig. 6A,B). Time course plots (Fig. 6E-H) show that a source of the ANOVA results was negative BOLD responses during the OL and OW in both groups of blind, but not sighted participants. However, sighted had slight positive BOLD responses in all but BA 47; these were more prominent during the OW task (Fig. 6). There were no responses during the BL task in any group. The MANOVA found that these differences were significant for all left hemisphere frontal regions when contrasting responses during the OL and OW tasks in blind compared to sighted participants (Table III); responses in right hemisphere regions also differed between EB and LB from NS during the OL task and for the OW task between EB and NS (Table III).

Parietal Cortex

All groups showed similar bilateral distributions of positive BOLD responses in anterior and lateral parietal cortex and no significant voxels for the ANOVA time-by-group factor. Despite widespread activity across the postcentral gyrus (BA 3, 1), peak responses were located within the S1 finger representation. All groups also showed increased activity bilaterally in the parietal operculum (BA 43), adjoining inferior supramarginal gyrus (BA 40), parietal cortex medial to the intraparietal sulcus (BA 5), and in the superior aspect of the supramarginal gyrus (BA 7).

DISCUSSION

The present results provide an example of reorganized visual cortex that involves cross-modal activation to tactile stimulation in blind people. Prior studies describe similar cross-modal tactile activation in blind humans [Burton et al., 2004; Gizewski et al., 2003; Sadato et al., 1996, 1998, 2002] and animals [Kahn and Krubitzer, 2002; Newton et al., 2002]. We found that tactile processing of embossed letters for both sublexical language tasks evoked greater bilateral activation of visual cortex in early and late blind compared to sighted people.

Visual cortex reorganization in blindness entails cross-modal activation within visual areas previously identified in sighted people. Furthermore, as discussed below, the most probable zones of activation in early and late blind people involved certain eccentricity bands within several lower tier visual areas and anterior projections of these bands into ventral and dorsal occipito-temporal cortex. The utilization of existing visual cortex architecture in blind

people is emphasized by evidence that the activated regions respect topographical domains, e.g., eccentricity bands.

Response Distributions in V1/V2

The posterior pole of occipital cortex (e.g., posterior V1/V2) was activated in all groups, even in sighted participants. This activation involved regions in V1/V2 that in sighted people normally reflect visual stimulation within a central gaze or foveal eccentricity representation [Grill-Spector and Malach, 2004]. Finding that tactile stimulation activates a comparable part of V1/V2 in blind and sighted people was surprising. However, engaging these posterior V1/V2 regions by tactile stimulation even in sighted people has been noted previously during a vibrotactile discrimination task [Burton et al., 2004]. Cross-modal activation of visual cortex (including V1) in sighted people may not be unique because such activity to tactile and auditory stimulation has been described after short-term visual deprivation [Pascual-Leone and Hamilton, 2001]. These findings collectively suggest that nonvisual inputs may activate visual cortex through some latent pathway. The functional relevance of this pathway following visual deprivation people is probably increased [Cohen et al., 1997; Hamilton et al., 2000; Pascual-Leone and Hamilton, 2001].

Blind people also showed V1 activity during stimulation with a moving smooth surface, a tactile task (BL) that we instructed the subjects to ignore. The evoked responses during the BL task were smaller than those to the letters. Prior studies suggested that cross-modal activation of reorganized visual cortex requires attention [Gizewski et al., 2003; Kujala et al., 2005; Sadato et al., 1996]. Although improbable and contrary to the instructions, the early blind participants might have attended to the smooth surface and thereby evoked the observed responses.

Lower Tier Extrastriate Visual Areas

In reference to visual area identifications in sighted people [Grill-Spector and Malach, 2004; Van Essen, 2004] and projections of regional borders to an averaged anatomy template [Van Essen, 2005], positive BOLD responses occurred in V2d, V3, and V3a superior to the calcarine sulcus, and VP and V4v inferior to the calcarine sulcus in early blind. The same areas were activated in late blind and suppressed in sighted participants. These responses suggest that in adapting to blindness, lower tier visual areas process tactile stimulation and that the potential for these cross-modal adaptations plausibly persist despite different ages of blindness onset.

The ANOVA map indicated that groups differed most within the parafoveal eccentricity band of lower tier visual areas. Responses in these regions were also generally larger and peaked earlier in EB compared to responses in LB. Parafoveal eccentricity band regions in sighted people are preferentially activated when distinguishing images of objects from textures despite varying views of the objects (e.g., altered sizes, shape distortions, colors, perspectives) [Hasson et al., 2002, 2003; Levy et al., 2004]. Thus, in sighted people prior studies have shown that parafoveal eccentricity band regions exhibit a more global response to objects that is unaffected by changes in specific visual features. The question is what might be processed in an anatomically analogous region in blind people. Speculatively, activation of a comparable region in blind people might indicate holistic processing of the embossed letters irrespective of fine-grain tactile shape features. Finding that EB had larger responses in parafoveal eccentricity regions compared to LB might plausibly indicate that EB processed each felt letter as a single object irrespective of detailed tactile features. Skill at more holistic processing in tactile reading of Braille has been noted more frequently in EB [Millar, 1987, 1997].

Higher Tier Visual Areas in Occipital Temporal Cortex

Group differences in the present results occurred in all VOT partitions previously identified in sighted people (i.e., V8 and BA 37/20 bilaterally). The V8 cortex involved the VOT partition (Fig. 4K) that in sighted people responds selectively when viewing faces and objects (Fig. 4K) [Hasson et al., 2002, 2003; Yovel and Kanwisher, 2004]. Viewing scenes preferentially activates the BA 37/20 cortex in sighted people [Levy et al., 2004]. Thus, no selectivity for a particular partition of VOT was found in blind people. However, group differences were based on larger positive BOLD responses in blind compared to sighted people, but positive BOLD responses in all groups possibly indicate that sighted and blind people might have utilized VOT similarly.

Prior studies suggested that letter identification in sighted people is a special case of object recognition [Flowers et al., 2004; Garrett et al., 2000; Polk et al., 2002; Puce et al., 1996; Tagamets et al., 2000]. The activation identified in these studies primarily was in left BA 37 in cortex that resides anterior to lower tier ventral visuotopic areas. In the present study, extensive commonality of activation across the groups in this more anterior temporal cortex lead to nearly complete absence of significant voxels bilaterally in the ANOVA map for group differences in much of BA 37. The only portion of BA 37 showing group differences was confined to a part of medial fusiform gyrus that was located just anterior to ventral visuotopic areas. In the left hemisphere this was posterior and medial (e.g., -31, -55, -14) to the regions previously identified with letter recognition tasks. Thus, the BA 37 region showing significantly larger BOLD responses in blind people did not coincide with the letter region of prior studies in sighted individuals. Despite these differences, the larger responses in VOT in blindness imply that the tactile processing of letters was enhanced in VOT. Unknown is whether these response enhancements might have contributed to the determination of “what” letter was touched in blind people. However, given prior reports of preferential activation for object viewing noted in these VOT regions in sighted people, the blind might plausibly have had enhanced processing of the tactile letters as objects.

In the present study, group differences were also noted in MT+ and LOC. Except for left MT+, group differences noted in MT+ and LOC activity was suppressed in sighted and manifested in blind people. Prior studies of these regions in sighted people have shown selective activation to visual images of faces and objects compared to textured surfaces [Hasson et al., 2002, 2003; Yovel and Kanwisher, 2004]. Hasson et al. also identified selective activation to viewing images of scenes in adjoining parts of nonvisuotopic BA 19. These authors collectively included these face, object, and scene partitions in a dorsal occipito-temporal cortex (DOT) that had a mirror symmetrical pattern of object representation to that noted in VOT. DOT regions have also been suggested to be part of a “where is it” pathway for object recognition [Hasson et al., 2002; Ungerleider and Haxby, 1994]. Unknown is whether the observed activity in blind people in similar DOT regions (e.g., MT+ and LOC) can be related to the object image selectivity functions proposed for these same regions in sighted people. Speculatively, the DOT activity in blind people might have reflected the focal localization of object critical tactile inputs on a single fingertip. Assessing this hypothesis, however, will require experiments in blind people that involve contrasting tactile stimulus locations and comparing tactile object to tactile texture recognition tasks.

Responses in Frontal and Temporal Cortex

Results showing group differences in frontal and temporal cortex possibly suggest that adaptive plasticity in blindness includes reorganization in nonvisual cortical areas. In nonvisual areas this plasticity might be reflected in the temporal dynamics of neuronal activity, which in the present study might have contributed to the earlier onset times to peak

BOLD responses detected in temporal cortex and negative BOLD responses in frontal cortex. The present results, however, cannot indicate whether enhanced performance, e.g., reaction time, noted especially in early blind people when identifying tactile letters, was causally related to the group differences in these nonvisual areas and/or to the presence of cross-modal activity in visual cortex.

Frontal cortex language areas—Prior studies in sighted people have shown that semantic and phonological language tasks increase activity in left inferior frontal regions corresponding to BA 44-47 in inferior and middle frontal gyri [Binder et al., 1997; Bookheimer, 2002; Demonet et al., 1992; Fiez, 1997; Fiez and Petersen, 1998; Gabrieli et al., 1998; McDermott et al., 2003; Paulesu et al., 1997; Petersen et al., 1989; Poldrack et al., 1999; Price, 2000; Roskies et al., 2001; Thompson-Schill et al., 1997]. In blind people, tactile encoding of letters led to large negative BOLD responses in these frontal cortex regions, which suggests suppression of lexical and sublexical processing when attending to tactile features associated with orthographic processing of block capital letters. In contrast, sighted showed small positive responses in BA 44-46, especially during the word task. The latter required accurate spelling of the generated word in order to know whether the selected word contained the identified letter. Thus, both tasks probably involved orthographic processing. The results in sighted people confirm prior findings that left frontal regions respond when viewing words, pseudowords, letter strings, or false-fonts, i.e., processes associated with general orthographic encoding [Tagamets et al., 2000]. Not all tasks that require attention to tactile stimulation suppress frontal language areas because flat responses were previously seen in these same language areas when blind people attended to vibrotactile stimulation that had no verbal components [Burton et al., 2004]. Yet, when reading Braille in conjunction with a semantic verb generation task, blind people activated left inferior frontal language areas to the same extent as predicted from studies with visually read nouns and verb generation in sighted people [Burton et al., 2002a]. The present findings might plausibly indicate an explicit suppression of frontal cortex language processes as an aid to discerning the embossed letters.

Temporal cortex—Visual and auditory activation of superior temporal sulcal (STS) cortex has been noted [Beauchamp et al., 2004a,b]. The present findings suggest that these multisensory properties include activation during tactile identification of letters. Prior reports hypothesized that multisensory STS regions integrate polysensory information associated with behaviorally relevant stimulation [Beauchamp et al., 2004a,b; Wright et al., 2003]. Beauchamp et al. [2004a] described a “patchy” distribution of activated foci for auditory, visual, and multisensory stimuli that extended ~2.5 cm along the length of left STS in single participants. We observed a similar length of three discrete foci in the time-by-group ANOVA in the right hemisphere that principally resulted from shorter latency and/or larger response peaks in early blind people. The ANOVA sites indicate foci where the groups responded differently to tactile inputs and are, therefore, not strictly comparable to foci activated by auditory and visual stimulation.

A developmental model proposed for cortical multisensory organization suggests that “auditory and visual inputs arrive in the STS-MS in separate patches, followed by integration in the intervening cortex” [Beauchamp et al., 2004a, p. 1192]. Several issues plausibly make this model relevant to group differences during tactile identification of letters. Integration of visual inputs into multisensory patches is impossible in EB completely blind from birth but presumably occurred in LB prior to blindness. Given that all groups showed overlapping locations for responses to tactile inputs in most of STS, it is probable that some multisensory patches similarly integrate tactile information. However, because LB experienced sight, their multisensory areas were probably formed with integration of auditory, visual, and tactile information, which is why the activation pattern in these people

resembles that obtained in sighted individuals. In EB, multisensory patches might only integrate tactile and auditory stimuli. In addition, EB may have a greater number of isolated tactile patches. These differences and a selectively activated focus in right anterior STS possibly underlie the BOLD responses in EB, with earlier elevations or peaks in foci where all groups showed positive BOLD responses. These distinctions indicate altered response dynamics for EB, which possibly reflects different utilization of tactile and/or multisensory “patches” in circumstances where there never was any visual input. Finding that EB identified letters faster might be a consequence of such earlier latency BOLD responses.

Acknowledgments

We thank Drs. D. Van Essen, A. Snyder, and M. McAvoy for analysis and data reconstruction software, and John Kreidler and Dr. G. Perry for design and construction of the tactile stimulator.

REFERENCES

- Aleman A, van Lee L, Mantione MH, Verkoijen IG, de Haan EH. Visual imagery without visual experience: evidence from congenitally totally blind people. *Neuroreport*. 2001; 12:2601–2604. [PubMed: 11496156]
- Amedi A, Raz N, Pianka P, Malach R, Zohary E. Early ‘visual’ cortex activation correlates with superior verbal memory performance in the blind. *Nat Neurosci*. 2003; 6:758–766. [PubMed: 12808458]
- Andersson JL, Sundin A, Valind S. A method for coregistration of PET and MR brain images. *J Nucl Med*. 1995; 36:1307–1315. [PubMed: 7790961]
- Arno P, De Volder AG, Vanlierde A, Wanet-Defalque MC, Strel E, Robert A, Sanabria-Bohorquez S, Veraart C. Occipital activation by pattern recognition in the early blind using auditory substitution for vision. *Neuroimage*. 2001; 13:632–645. [PubMed: 11305892]
- Beauchamp MS, Argall BD, Bodurka J, Duyn JH, Martin A. Unraveling multisensory integration: patchy organization within human STS multisensory cortex. *Nat Neurosci*. 2004a; 7:1190–1192. [PubMed: 15475952]
- Beauchamp MS, Lee KE, Argall BD, Martin A. Integration of auditory and visual information about objects in superior temporal sulcus. *Neuron*. 2004b; 41:809–823. [PubMed: 15003179]
- Binder JR, Frost JA, Hammeke TA, Cox RW, Rao SM, Prieto T. Human brain language areas identified by functional magnetic resonance imaging. *J Neurosci*. 1997; 17:353–362. [PubMed: 8987760]
- Bookheimer S. Functional MRI of language: new approaches to understanding the cortical organization of semantic processing. *Annu Rev Neurosci*. 2002; 25:151–188. [PubMed: 12052907]
- Boynton GM, Engel SA, Glover GH, Heeger DJ. Linear systems analysis of functional magnetic resonance imaging in human V1. *J Neurosci*. 1996; 16:4207–4221. [PubMed: 8753882]
- Büchel C, Price C, Frackowiak RS, Friston K (1998): Different activation patterns in the visual cortex of late and congenitally blind subjects. *Brain*. 121:409–419. [PubMed: 9549517]
- Burton H, Snyder AZ, Conturo TE, Akbudak E, Ollinger JM, Raichle ME. Adaptive changes in early and late blind: an fMRI study of Braille reading. *J Neurophysiol*. 2002a; 87:589–611. [PubMed: 11784773]
- Burton H, Snyder AZ, Diamond J, Raichle ME. Adaptive changes in early and late blind: an fMRI study of verb generation to heard nouns. *J Neurophysiol*. 2002b; 88:3359–3371. [PubMed: 12466452]
- Burton H, Diamond JB, McDermott KB. Dissociating cortical regions activated by semantic and phonological tasks to heard words: an fMRI study in blind and sighted individuals. *J Neurophysiol*. 2003; 90:1965–1982. [PubMed: 12789013]
- Burton H, Sinclair R, McLaren D. Cortical activity to vibrotactile stimulation: an fMRI study in blind and sighted individuals. *Hum Brain Mapp*. 2004; 23:210–228. [PubMed: 15449356]

- Cohen LG, Celnik P, Pascual-Leone A, Corwell B, Faiz L, Dambrosia J, Honda M, Sadato N, Gerloff C, Catala MD. Functional relevance of cross-modal plasticity in blind humans. *Nature*. 1997; 389:180–183. [PubMed: 9296495]
- Dale AM, Buckner RL. Selective averaging of rapidly presented individual trials using fMRI. *Hum Brain Mapp*. 1997; 5:329–340. [PubMed: 20408237]
- Demonet JF, Chollet F, Ramsay S, Cardebat D, Nespoulous JL, Wise R, Rascol A, Frackowiak R. The anatomy of phonological and semantic processing in normal subjects. *Brain*. 1992; 115:1753–1768. [PubMed: 1486459]
- Dumoulin SO, Bittar RG, Kabani NJ, Baker CL Jr, Le Goualher G, Bruce Pike G, Evans AC. A new anatomical landmark for reliable identification of human area V5/MT: a quantitative analysis of sulcal patterning. *Cereb Cortex*. 2000; 10:454–463. [PubMed: 10847595]
- Fiez JA. Phonology, semantics, and the role of the left inferior prefrontal cortex. *Hum Brain Mapp*. 1997; 5:79–83. [PubMed: 10096412]
- Fiez JA, Petersen SE. Neuroimaging studies of word reading. *Proc Natl Acad Sci U S A*. 1998; 95:914–921. [PubMed: 9448259]
- Flowers DL, Jones K, Noble K, VanMeter J, Zeffiro TA, Wood FB, Eden GF. Attention to single letters activates left extrastriate cortex. *Neuroimage*. 2004; 21:829–839. [PubMed: 15006649]
- Forman SD, Cohen JD, Fitzgerald M, Eddy WF, Mintun MA, Noll DC. Improved assessment of significant activation in functional magnetic resonance imaging (fMRI): use of a cluster-size threshold. *Magn Reson Med*. 1995; 33:636–647. [PubMed: 7596267]
- Friston K, Ashburner J, Poline J, Frith C, Heather J, Frackowiak R. Spatial registration and normalization of images. *Hum Brain Mapp*. 1995a; 2:165–189.
- Friston K, Holmes A, Worsley K, Poline J, Frith C, Frackowiak R. Statistical parametric maps in functional imaging: a general linear approach. *Hum Brain Mapp*. 1995b; 2:189–210.
- Gabrieli JD, Poldrack RA, Desmond JE. The role of left prefrontal cortex in language and memory. *Proc Natl Acad Sci U S A*. 1998; 95:906–913. [PubMed: 9448258]
- Garrett AS, Flowers DL, Absher JR, Fahey FH, Gage HD, Keyes JW, Porrino LJ, Wood FB. Cortical activity related to accuracy of letter recognition. *Neuroimage*. 2000; 11:111–123. [PubMed: 10679184]
- Gizewski ER, Gasser T, de Greiff A, Boehm A, Forsting M. Cross-modal plasticity for sensory and motor activation patterns in blind subjects. *Neuroimage*. 2003; 19:968–975. [PubMed: 12880825]
- Gougoux F, Zatorre RJ, Lassonde M, Voss P, Lepore F. A functional neuroimaging study of sound localization: visual cortex activity predicts performance in early-blind individuals. *PLoS Biol*. 2005; 3:e27. [PubMed: 15678166]
- Grill-Spector K, Malach R. The human visual cortex. *Annu Rev Neurosci*. 2004; 27:649–677. [PubMed: 15217346]
- Hadjikhani N, Liu AK, Dale AM, Cavanagh P, Tootell RB. Retinotopy and color sensitivity in human visual cortical area V8. *Nat Neurosci*. 1998; 1:235–241. [PubMed: 10195149]
- Hajnal JV, Saeed N, Soar EJ, Oatridge A, Young IR, Bydder GM. A registration and interpolation procedure for subvoxel matching of serially acquired MR images. *J Comput Assist Tomogr*. 1995; 19:289–296. [PubMed: 7890857]
- Hamilton R, Keenan JP, Catala M, Pascual-Leone A. Alexia for Braille following bilateral occipital stroke in an early blind woman. *Neuroreport*. 2000; 11:237–240. [PubMed: 10674462]
- Hasson U, Levy I, Behrmann M, Hendler T, Malach R. Eccentricity bias as an organizing principle for human high-order object areas. *Neuron*. 2002; 34:479–490. [PubMed: 11988177]
- Hasson U, Harel M, Levy I, Malach R. Large-scale mirror-symmetry organization of human occipito-temporal object areas. *Neuron*. 2003; 37:1027–1041. [PubMed: 12670430]
- Kahn DM, Krubitzer L. Massive cross-modal cortical plasticity and the emergence of a new cortical area in developmentally blind mammals. *Proc Natl Acad Sci U S A*. 2002; 99:11429–11434. [PubMed: 12163645]
- Kanwisher N, McDermott J, Chun MM. The fusiform face area: a module in human extrastriate cortex specialized for face perception. *J Neurosci*. 1997; 17:4302–4311. [PubMed: 9151747]

- Kujala T, Palva MJ, Salonen O, Alku P, Huutilainen M, Jarvinen A, Naatanen R. The role of blind humans' visual cortex in auditory change detection. *Neurosci Lett*. 2005; 379:127–131. [PubMed: 15823429]
- Lambert S, Sampaio E, Mauss Y, Scheiber C. Blindness and brain plasticity: contribution of mental imagery? An fMRI study. *Cogn Brain Res*. 2004; 20:1–11.
- Lancaster JL, Glass TG, Lankipalli BR, Downs H, Mayberg H, Fox PT. A modality-independent approach to spatial normalization of tomographic images of the human brain. *Hum Brain Mapp*. 1995; 3:209–223.
- Levy I, Hasson U, Avidan G, Hendler T, Malach R. Center-periphery organization of human object areas. *Nat Neurosci*. 2001; 4:533–539. [PubMed: 11319563]
- Levy I, Hasson U, Harel M, Malach R. Functional analysis of the periphery effect in human building related areas. *Hum Brain Mapp*. 2004; 22:15–26. [PubMed: 15083523]
- Loomis JM. On the tangibility of letters and braille. *Percept Psychophys*. 1981; 29:37–46. [PubMed: 7243529]
- Malach R, Reppas JB, Benson RR, Kwong KK, Jiang H, Kennedy WA, Ledden PJ, Brady TJ, Rosen BR, Tootell RB. Object-related activity revealed by functional magnetic resonance imaging in human occipital cortex. *Proc Natl Acad Sci U S A*. 1995; 92:8135–8139. [PubMed: 7667258]
- Malach R, Levy I, Hasson U. The topography of high-order human object areas. *Trends Cogn Sci*. 2002; 6:176–184. [PubMed: 11912041]
- McDermott K, Petersen S, Watson J, Ojemann J. A procedure for identifying regions preferentially activated by attention to semantic and phonological relations using functional magnetic resonance imaging. *Neuropsychologia*. 2003; 41:293–303. [PubMed: 12457755]
- Melzer P, Morgan VL, Pickens DR, Price RR, Wall RS, Ebner FF. Cortical activation during Braille reading is influenced by early visual experience in subjects with severe visual disability: a correlational fMRI study. *Hum Brain Mapp*. 2001; 14:186–195. [PubMed: 11559962]
- Miezin FM, Maccotta L, Ollinger JM, Petersen SE, Buckner RL. Characterizing the hemodynamic response: effects of presentation rate, sampling procedure, and the possibility of ordering brain activity based on relative timing. *Neuroimage*. 2000; 11:735–759. [PubMed: 10860799]
- Millar S. Perceptual and task factors in fluent braille. *Perception*. 1987; 16:521–536. [PubMed: 3444732]
- Millar, S. *Reading by touch*. Routledge; London: 1997.
- Mugler JPD, Brookeman JR. Three-dimensional magnetization-prepared rapid gradient-echo imaging (3D MP RAGE). *Magn Reson Med*. 1990; 15:152–157. [PubMed: 2374495]
- Nelles J, Lugar H, Coalson R, Miezin FM, Petersen SE, Schlaggar B. An automated method for extracting response latencies of subject vocalizations in event-related fMRI experiments. *Neuron*. 2003 in press.
- Newton JR, Sikes RW, Skavenski AA. Cross-modal plasticity after monocular enucleation of the adult rabbit. *Exp Brain Res*. 2002; 144:423–429. [PubMed: 12037628]
- Ojemann JG, Akbudak E, Snyder AZ, McKinstry RC, Raichle ME, Conturo TE. Anatomic localization and quantitative analysis of gradient refocused echo-planar fMRI susceptibility artifacts. *Neuroimage*. 1997; 6:156–167. [PubMed: 9344820]
- Ollinger JM, Corbetta M, Shulman GL. Separating processes within a trial in event-related functional MRI. I. The method. *Neuroimage*. 2001a; 13:210–217. [PubMed: 11133323]
- Ollinger JM, Corbetta M, Shulman GL. Separating processes within a trial in event-related functional MRI. II. Analysis. *Neuroimage*. 2001b; 13:218–229. [PubMed: 11133324]
- Pascual-Leone A, Hamilton R. The metamodal organization of the brain. *Prog Brain Res*. 2001; 134:427–445. [PubMed: 11702559]
- Paulesu E, Goldacre B, Scifo P, Cappa S, Gilardi M, Castiglioni I, Perani D, Fazio F. Functional heterogeneity of left inferior frontal cortex as revealed by fMRI. *Neuroreport*. 1997; 8:2011–2016. [PubMed: 9223094]
- Petersen SE, Fox PT, Posner MI, Mintun MA, Raichle ME. Positron emission tomographic studies of the processing of single words. *J Cogn Neurosci*. 1989; 1:153–170.

- Poldrack RA, Wagner AD, Prull MW, Desmond JE, Glover GH, Gabrieli JD. Functional specialization for semantic and phonological processing in the left inferior prefrontal cortex. *Neuroimage*. 1999; 10:15–35. [PubMed: 10385578]
- Polk TA, Stallcup M, Aguirre GK, Alsop DC, D’Esposito M, Detre JA, Farah MJ. Neural specialization for letter recognition. *J Cogn Neurosci*. 2002; 14:145–159. [PubMed: 11970782]
- Price CJ. The anatomy of language: contributions from functional neuroimaging. *J Anat*. 2000; 197:335–359. [PubMed: 11117622]
- Puce A, Allison T, Asgari M, Gore JC, McCarthy G. Differential sensitivity of human visual cortex to faces, letterstrings, and textures: a functional magnetic resonance imaging study. *J Neurosci*. 1996; 16:5205–5215. [PubMed: 8756449]
- Raczkowski D, Kalat JW, Nebes R. Reliability and validity of some handedness questionnaire items. *Neuropsychologia*. 1974; 12:43–47. [PubMed: 4821188]
- Rakic P. Specification of cerebral cortical areas. *Science*. 1988; 241:170–176. [PubMed: 3291116]
- Röder B, Rösler F, Neville HJ. Auditory memory in congenitally blind adults: a behavioral-electrophysiological investigation. *Cogn Brain Res*. 2001; 11:289–303.
- Röder B, Stock O, Bien S, Neville H, Rosler F. Speech processing activates visual cortex in congenitally blind humans. *Eur J Neurosci*. 2002; 16:930–936. [PubMed: 12372029]
- Roskies AL, Fiez JA, Balota DA, Raichle ME, Petersen SE. Task-dependent modulation of regions in the left inferior frontal cortex during semantic processing. *J Cogn Neurosci*. 2001; 13:829–843. [PubMed: 11564326]
- Sadato N, Pascual-Leone A, Grafman J, Ibanez V, Deiber MP, Dold G, Hallett M. Activation of the primary visual cortex by Braille reading in blind subjects. *Nature*. 1996; 380:526–528. [PubMed: 8606771]
- Sadato N, Pascual-Leone A, Grafman J, Deiber MP, Ibanez V, Hallett M. Neural networks for Braille reading by the blind. *Brain*. 1998; 121:1213–1229. [PubMed: 9679774]
- Sadato N, Okada T, Honda M, Yonekura Y. Critical period for cross-modal plasticity in blind humans: a functional MRI study. *Neuroimage*. 2002; 16:389–400. [PubMed: 12030824]
- Snyder, AZ. Difference image vs. ratio image error function forms in PET-PET realignment. In: Bailey D, Jones T, editors. *Quantification of brain function using PET*. Academic Press; San Diego: 1996. p. 131-137.
- Tagamets MA, Novick JM, Chalmers ML, Friedman RB. A parametric approach to orthographic processing in the brain: an fMRI study. *J Cogn Neurosci*. 2000; 12:281–297. [PubMed: 10771412]
- Talairach, J.; Tournoux, P. *Coplanar stereotaxic atlas of the human brain*. Thieme Medical; New York: 1988.
- Thompson-Schill SL, D’Esposito M, Aguirre GK, Farah MJ. Role of left inferior prefrontal cortex in retrieval of semantic knowledge: a reevaluation. *Proc Natl Acad Sci U S A*. 1997; 94:14792–14797. [PubMed: 9405692]
- Uhl F, Franzen P, Lindinger G, Lang W, Deecke L. On the functionality of the visually deprived occipital cortex in early blind persons. *Neurosci Lett*. 1991; 124:256–259. [PubMed: 2067724]
- Ungerleider LG, Haxby JV. ‘What’ and ‘where’ in the human brain. *Curr Opin Neurobiol*. 1994; 4:157–165. [PubMed: 8038571]
- Van Essen, DC. Organization of visual areas in macaque and human cerebral cortex. In: Chalupa, L.; Werner, JS., editors. *The visual neurosciences*. MIT Press; Cambridge, MA: 2004. p. 507-521.
- Van Essen DC. A population-average, landmark- and surface-based (PALS) atlas of human cerebral cortex. *Neuroimage*. 2005 in press.
- Vanlierde A, De Volder AG, Wanet-Defalque MC, Veraart C. Occipito-parietal cortex activation during visuo-spatial imagery in early blind humans. *Neuroimage*. 2003; 19:698–709. [PubMed: 12880800]
- Vega-Bermudez F, Johnson KO, Hsiao SS. Human tactile pattern recognition: active versus passive touch, velocity effects, and patterns of confusion. *J Neurophysiol*. 1991; 65:531–546. [PubMed: 2051193]
- Woods RP, Mazziotta JC, Cherry SR. MRI-PET registration with automated algorithm. *J Comput Assist Tomogr*. 1993; 17:536–546. [PubMed: 8331222]

- Wright TM, Pelphrey KA, Allison T, McKeown MJ, McCarthy G. Polysensory interactions along lateral temporal regions evoked by audiovisual speech. *Cereb Cortex*. 2003; 13:1034–1043. [PubMed: 12967920]
- Yovel G, Kanwisher N. Face perception: domain specific, not process specific. *Neuron*. 2004; 44:889–898. [PubMed: 15572118]
- Zarahn E, Aguirre G, D’Esposito M. A trial-based experimental design for fMRI. *Neuroimage*. 1997; 6:122–138. [PubMed: 9299386]
- Zatorre RJ. Do you see what I’m saying? Interactions between auditory and visual cortices in cochlear implant users. *Neuron*. 2001; 31:13–14. [PubMed: 11498046]

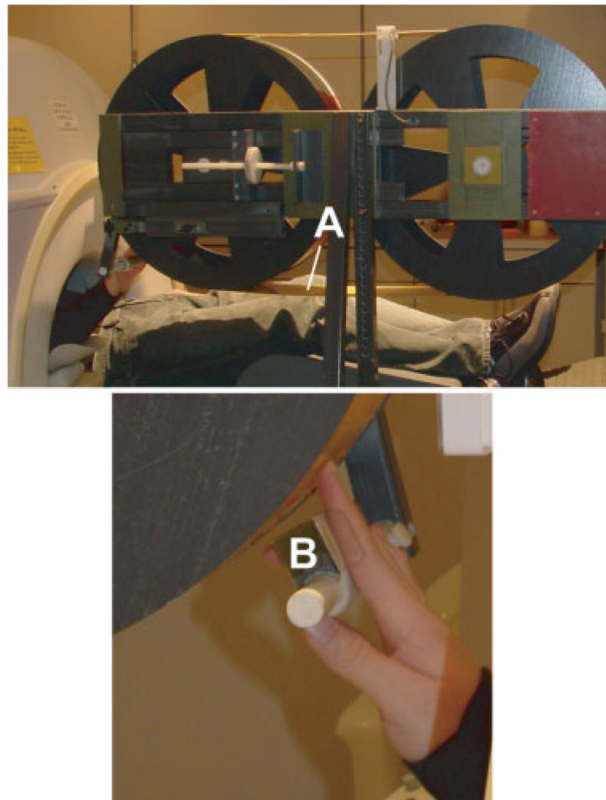


Figure 1.

The rotating drum device used to passively translate embossed capital letters against the right index fingertip from proximal to distal. The device was constructed using two fiberglass wheels and a connecting belt (A) that consists of a flexible photopolymer printing material embossed with five tracks of block capital letters using a commercial photo etching process (B.W. Johnson, Joplin, MO). An adjustable finger/hand rest (B) aligned the fingertip over a selected track for each imaging run.

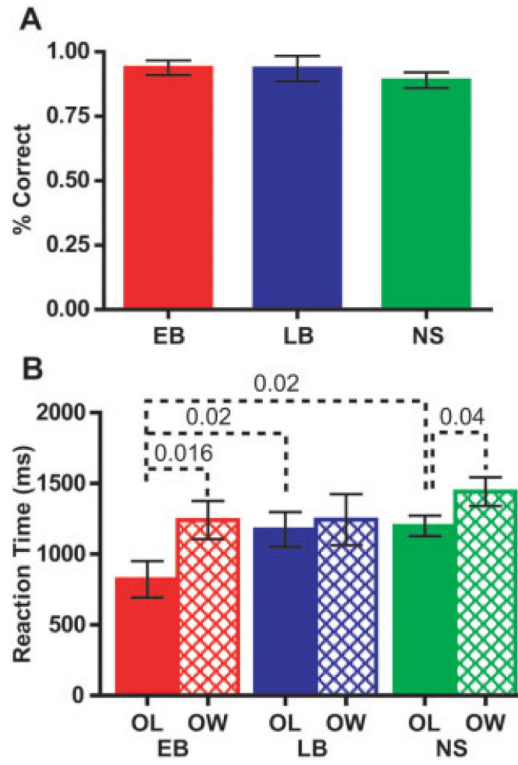


Figure 2. Accuracy and reaction times for early (EB), late (LB) blind, and sighted (NS) people were obtained during fMRI. **A:** Proportion of letters correctly identified during the overt letter task (mean and SEM). **B:** Reaction times (mean and SEM) to all responses were measured from the peak of the voiced response to the end of rotation of each letter string in overt letter (OL) and word (OW) tasks. Dashed lines labeled with *P*-values connect significant Mann-Whitney *U*-test or Wilcoxon matched pairs test.

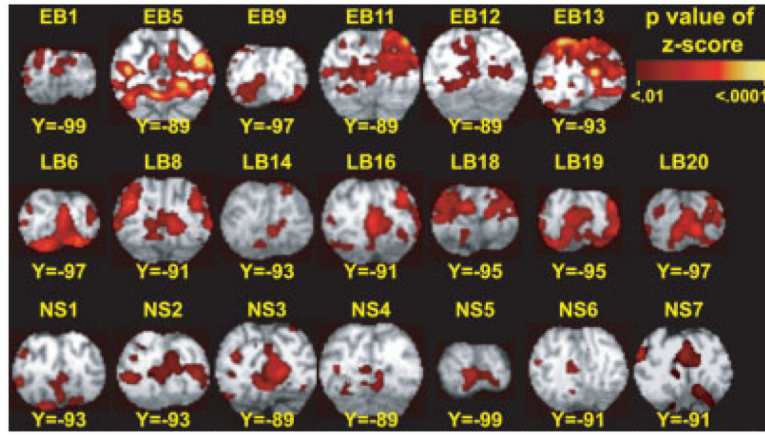


Figure 3. Distribution of increased activity is shown for a posterior occipital portion of V1. Results are shown from individuals with suprathreshold responses. Images are multiple-comparison corrected cross-correlation z-score maps (minimum $z = 4$, two face-connected voxels) overlaid onto atlas transformed [Talairach and Tournoux, 1988] structural anatomy for each individual. Labels cross-reference to demographic characteristics listed in Table I (early blind, EB; late blind, LB; and sighted, NS).

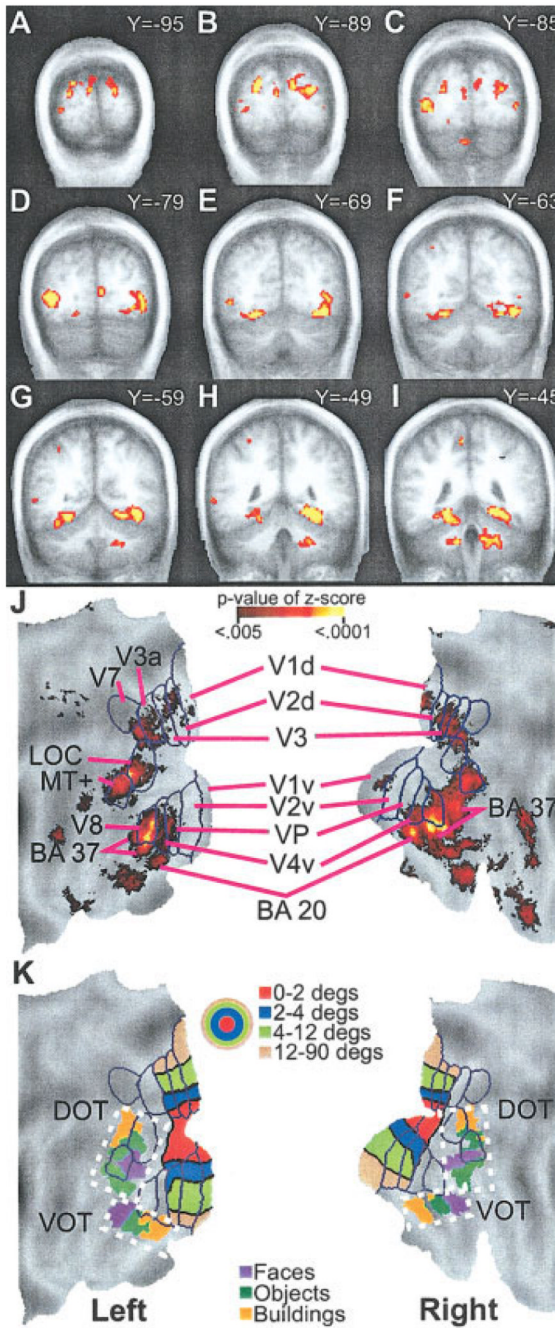


Figure 4. Distribution of multiple comparison corrected z-scores of significant F-ratios for the ANOVA time-by-group factor are shown on selected coronal sections (A-I) and surface-based reconstruction of the occipito-temporal cortex (J). Scale for P-values of z-scores shows range for images illustrated in A-J. Surface anatomy created using a population-average landmark-linked and surface-based atlas [PALS; Van Essen, 2005]. J: Projection of borders onto PALS and labeling of visual areas are from prior identifications in sighted people [Hadjikhani et al., 1998; Van Essen, 2004]. K: Projection of eccentricity bands for lower tier visual areas onto PALS. Color scale in concentric circles shows different degrees

of eccentricity. Foveal to peripheral eccentricity bands in the surface-based reconstruction align from the bottom to the top in dorsal visual areas and from the top to the bottom in ventral visual areas. In the volume images (**A-I**), foveal to peripheral ordering of eccentricity bands occupies, respectively, posterior to anterior Talairach atlas coordinates. In addition, object selective regions in ventral and dorsal occipito-temporal cortex (VOT and DOT) were projected onto PALS using spheres centered on previously reported centers-of-mass coordinates [Hasson et al., 2002]. The color scale shown by boxes indicates regions activated when viewing different objects. Hasson et al. proposed for sighted people a hypothetical scheme for foveal/central gaze, parafoveal, and peripheral eccentricity bands related, respectively, to face, object, and scene activated regions [Hasson et al., 2002]. Brodmann area, BA; dorsal and ventral occipito-temporal cortex, DOT and VOT; lateral occipital complex, LOC; medial temporal area, MT; dorsal and ventral primary visual areas, V1d, V1v; dorsal and ventral second visual areas, V2d, V2v; third visual areas, V3, V3a; ventral fourth visual area, V4v; ventral posterior visual area, VP; seventh visual area, V7; eighth visual area, V8.

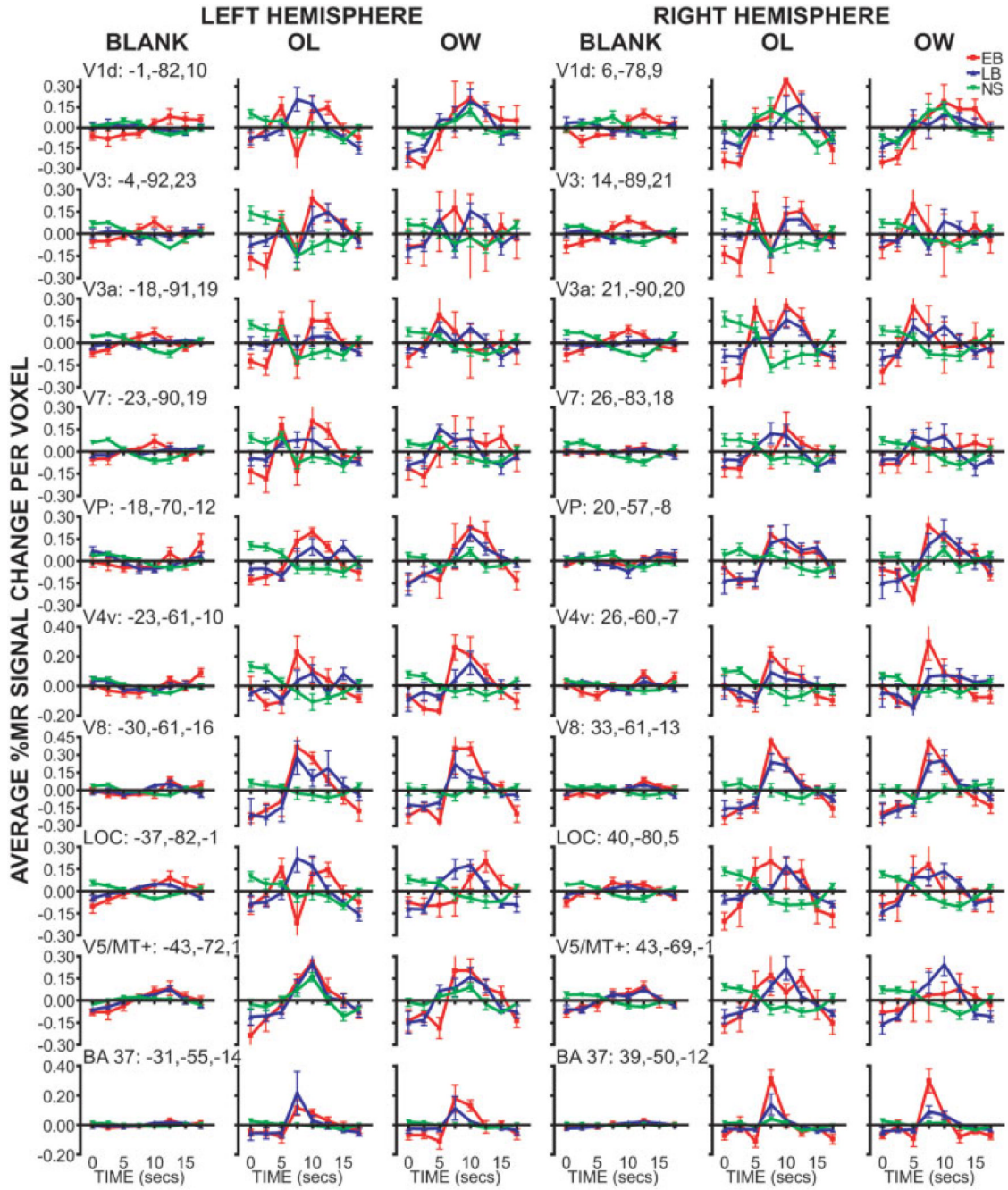


Figure 5. Time course plots for occipito-temporal ROIs identified from the ANOVA time-by-group factor. Data at each time point shows group mean and SEM (early blind, EB; late blind, LB; and sighted, NS). Each column shows data obtained during a different task (BLANK, passive stimulation with a moving smooth surface; OL, stating the identified letter, OW, stating a verb that contains the identified letter). Atlas coordinate locations are listed for peak, based on a center-of-mass calculation, z-score of the ANOVA time-by-group factor. Abbreviations: see Figure 4.

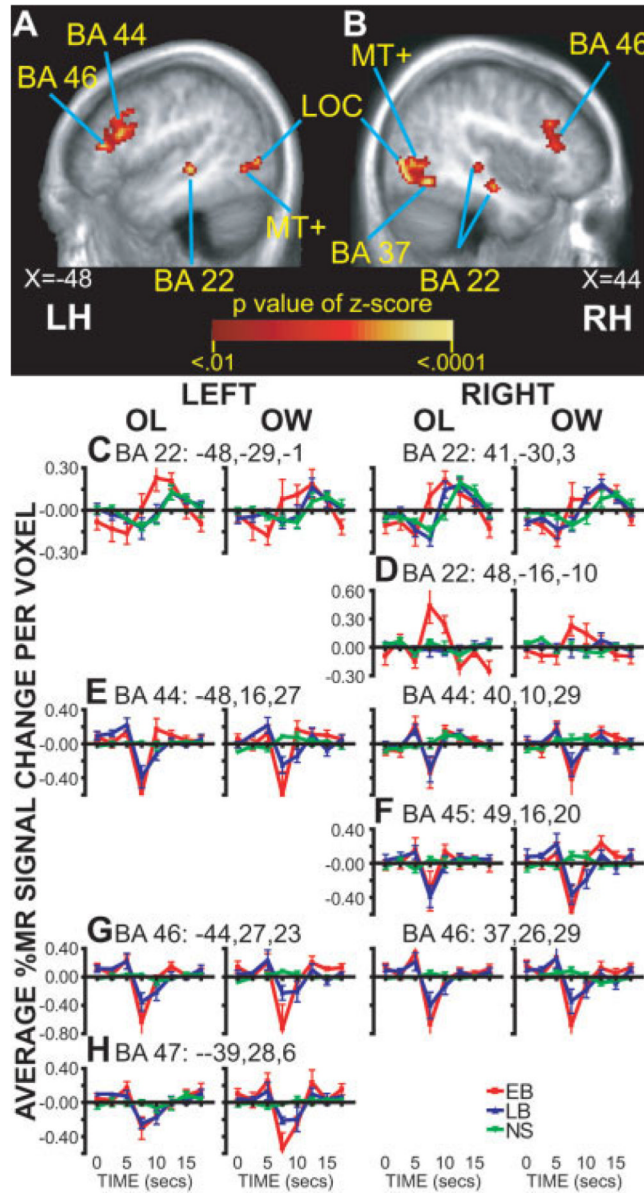


Figure 6. ROIs in the temporal and frontal cortex. **A,B:** Selected sagittal sections of the ANOVA time-by-group factor. **C,D:** Time course plots for regions in temporal cortex BA 22. **E-H:** Time course plots for frontal cortex regions in BA 44-47. Data at each time point shows group mean and SEM (early blind, EB; late blind, LB; and sighted, NS). Each column shows data obtained during a different task (OL, overt letter identification, OW, overt word whose spelling includes identified letter). Atlas coordinate locations are listed for peak, based on a center-of-mass calculation for the ANOVA time-by-group factor z-score. Abbreviations: see Figure 4.

TABLE 1

Demographic characteristics of blind and sighted participants

ID	Age (yr)	Sex	Right-handed (%)	Reading hand	w.p.m.	Age of onset (yr)	Light sensitivity	Years reading	Cause of blindness	Correct (%)	RT letters (ms)	RT words (ms)
Early 1	54	F	100	Both	170.6	0	None	49	Retinopathy of prematurity	100	350.0	1,138.2
Early 5	44	F	100	Both	88.1	3	None	38	Glaucoma	95	776.5	1,060.6
Early 7	72	M	94	Both	40.4	5	None	66	Cataracts	100	819.1	1,302.5
Early 9	49	M	80	Right	113.3	0	None	44	Retrolental fibroplasia	95	735.6	899.5
Early 10	37	M	90	Both	71.2	0	Presence	32	Retinopathy of prematurity	100		
Early 11	28	M	95	Left	58.7	0	Some	21	Leber's congenital amaurosis	100	1,480.0	1,858.5
Early 12	27	M	91	Left	60.2	0	None	22	Retinopathy of prematurity	100	926.8	
Early 13	71	F	75	Both	109.2	0	None	65	Eye infection	84		
Early 14	59	F	91	Both	137	0	Light source	54	Genetic retinal pigmentation	100	665.7	1,182.0
Average	49.0		90.7		94.3	0.9		43.4		97.1	822.0	1,240.2
SEM (±)	5.6		2.8		14.0	0.6		5.6		1.8	113.9	110.4
Late 6	51	F	100	Right	37.6	25	None	24	Retinitis pigmentosa	100		
Late 8	51	F	100	Both	32.6	12	Right eye	14	Steven Johnson's syndrome	95	1,511.0	1,417.7
Late 11	48	F	23	Both	182.3	20	Right eye	42	Retinopathy of prematurity	NR		
Late 14	19	M	87	Left	71.7	18	Some	13	Microcomea	100	1,038.6	1,085.1
Late 16	41	M	100	Both	37.5	11	None	30	Cataracts	100		
Late 17	23	M	100	Both	76.6	5.5	Some	17	Detached retina	100		
Late 18	61	F	100	Left	10.0	41	Some	5	Retinitis pigmentosa	89.5		
Late 19	58	F	91	Right	50.0	7	Some	9 months	Macular degeneration	84.2	949.7	825.7
Late 20	42	F	100	Both	106.3	7	None	34	Glaucoma	95	1,194.5	1,645.1
Average	43.8				67.2	16.3		22.4		95.5	1,173.4	1,243.4
SEM (±)	4.8				17.2	3.8		4.1		2.2	93.3	136.5
Sighted 1	62	M	73							63	1,426.2	1,925.7
Sighted 2	52	F	91							95	1,230.0	1,262.9
Sighted 3	56	M	86							100	785.4	1,550.6
Sighted 4	36	M	86							100		
Sighted 5	33	M	36							100	1,142.5	1,299.8

ID	Age (yr)	Sex	Right-handed (%)	Reading hand	w.p.m.	Age of onset (yr)	Light sensitivity	Years reading	Cause of blindness	Correct (%)	RT letters (ms)	RT words (ms)
Sighted 6	48	F	95							74	1,074.8	1,573.0
Sighted 7	26	M	100							89.5		
Sighted 8	68	M	14							95	1,258.7	1,107.3
Sighted 9	18	M	-100							95	1,303.0	
Sighted 10	33	F	23							100	1,378.6	1,381.2
Average	43.2									91.2	1,199.9	1,442.9
SEM (\pm)	5.2									4.0	64.2	84.7

TABLE II
F-test probability values from **MANOVA** for occipital-temporal time-by-group **ANOVA** regions

Region*	x, y, z	Defined volume (mm ³)	EBvsNS			LBvsNS			EBvsLB		
			BL	OL	OW	BL	OL	OW	BL	OL	OW
V1d	-1, -82,10	1,224	0.034	<0.0001	0.031	0.036	0.013	—	—	—	
V2d	-2, -86,14	1,496	<0.001	<0.0001	0.02	0.048	—	—	0.005	—	
V3	-4, -92,23	1,456	0.002	<0.0001	0.041	0.014	0.023	—	0.008	—	
V3a	-18, -91,19	2,608	<0.001	<0.0001	0.027	0.01	0.029	—	0.003	—	
V7	-23, -90,19	1,336	0.007	0.003	—	<0.0001	0.01	—	0.008	—	
VP	-18, -70, -12	3,000	—	<0.0001	0.001	0.02	<0.0001	0.048	—	0.038	
V4v	-23, -61, -10	1,704	0.042	<0.0001	<0.0001	—	0.022	—	0.014	0.035	
V8	-30, -61, -16	2,200	0.032	<0.0001	<0.0001	0.025	0.018	0.007	—	—	
LOC V5/	-37, -82, -1	3,408	<0.0001	<0.0001	<0.0001	<0.0001	0.010	<0.0001	—	0.001	
MT+	-43, -72,1	2,256	—	0.019	<0.0001	<0.0001	—	—	—	0.004	
BA20	-29, -30, -21	9,216	0.005	0.004	<0.0001	—	0.023	0.015	0.0049	—	
BA37	-31, -55, -14	3,272	—	0.004	<0.0001	—	—	—	—	—	
RH											
V1d	6, -78,9	1,248	0.021	<0.0001	0.026	—	0.005	—	—	—	
V2d	12, -90,17	1,736	<0.0001	<0.0001	—	<0.0001	0.02	—	0.028	—	
V3	14, -89,21	1,520	<0.0001	<0.0001	<0.0001	0.012	0.009	—	0.01	—	
V3a	21, -90,20	2,152	<0.0001	0.0001	0.001	0.002	0.0001	0.003	—	—	
V7	26, -83,18	712	0.007	<0.0001	—	<0.0001	0.031	0.003	—	—	
V1v	7, -76,6	1,408	0.043	<0.0001	0.005	0.049	0.011	—	—	—	
VP	20, -57, -8	776	0.003	<0.0001	0.010	0.004	0.002	—	—	—	
V4v	26, -60, -7	2,152	0.003	<0.0001	<0.0001	0.001	0.015	—	—	0.045	
V8	33, -61, -13	2,760	0.016	<0.0001	<0.0001	0.02	<0.0001	0.009	—	—	
LOC V5/	40, -80, 5	3,272	0.0002	<0.0001	0.011	0.006	<0.0001	<0.0001	—	—	
MT+	43, -69, -1	2,080	<0.0001	<0.0001	0.006	<0.0001	0.001	<0.0001	—	—	
BA20	38, -22, -20	12,456	—	<0.0001	<0.0001	0.022	0.049	—	—	—	
BA37	39, -50, -12	8,984	—	<0.0001	<0.0001	0.012	—	—	—	0.023	

* LH V1v had no differences between groups; LH and RH V2v had no differences between groups. BA, Brodmann Area; MT+, middle temporal area; LOC, lateral occipital area; —, not significant.

TABLE III

F-test probability values from MANOVA by region

	Brodmann area	x, y, z	Defined volume (mm ³)	EBvsNS			LBvsNS			EBvsLB			
				BL	OL	OW	BL	OL	OW	BL	OL	OW	
Frontal cortex													
	LH	BA44	-48,16,27	4,424	—	0.001	0.012	—	<0.0001	0.01	—	—	0.007
		BA46	-44,27,23	6,080	—	0.037	0.004	—	0.002	0.016	—	—	—
		BA47	-39,28,6	984	—	0.024	0.029	—	0.013	<0.0001	—	—	—
	RH	BA44	40,10,29	4,656	—	0.016	0.023	—	0.016	—	—	—	—
		BA45	49,16,20	2,552	—	0.016	0.018	—	<0.0001	—	—	—	—
		BA46	37,26,29	8,496	—	0.001	0.009	—	0.033	—	—	0.035	—
Temporal cortex													
	LH	BA22	-48,-29,-1	1,872	—	0.019	—	—	—	—	—	—	—
	RH	BA22	41,-30,3	1,032	—	0.007	0.022	—	—	—	—	0.027	—
		BA22	50,-23,-1	2,152	—	0.009	0.003	—	—	—	—	0.006	—
		BA22	48,-16,-10	1,000	—	0.015	<0.0001	—	—	—	—	0.002	—

—, not significant.